3426 *Chem. Mater.* **2010,** *22,* 3426–3432
DOI:10.1021/cm1004278

CHEMISTRY OF MATERIALS
Article

Electrochemical Generation of Thin Silica Films with Hierarchical Porosity

Mathieu Etienne,*[,†] Sébastien Sallard,[‡] Michael Schröder,[‡] Yann Guillemin,[†] Simone Mascotto,[‡] Bernd M. Smarsly,[‡] and Alain Walcarius[†]

[†]*Laboratoire de Chimie Physique et Microbiologie pour l'Environnement, UMR 7564, CNRS − Institut Jean Barriol − Nancy-Université, 405, rue de Vandœuvre, 54600 Villers-lès-Nancy, France, and* [‡]*Physikalisch-Chemisches Institut, Justus-Liebig-Universität Giessen, Heinrich-Buff-Ring 58, Giessen D-35392, Germany*

Received February 10, 2010. Revised Manuscript Received April 20, 2010

Thin films with combined macropores (∼100 nm) and mesopores (∼3 nm) can be prepared by the electro-assisted deposition of a mesoporous silica material inside a polystyrene bead assembly. The filling of voids between the polystyrene beads template strongly depends on the deposition time, as demonstrated by systematic SEM analysis. Low deposition time leads only to very thin silica layers on the PS beads. Longer deposition time leads to the complete filling of the macroporous texture and to the growth of an additional overlayer with very well oriented pores normal to the electrode surface. The presence of mesopores into the film has been evidenced with using TEM, grazing incidence X-ray diffraction (GIXD), and Krypton sorption isotherm. The electrochemical characterization demonstrates that the hierarchical material is highly permeable to external reagents, being thereby promising for various applications involving such mass transport processes.

1. Introduction

Multiscale porosity control in functional materials is a major field of investigation, and it concerns numerous applications, including catalysis, separation science, drug delivery, electrode material for fuel cells, and sensing.[1−4] Rational control of matter and functionality over different length scales and/or pore dimensions to generate hierarchical systems is highly desired because it contributes to improve properties of porous materials.[5] For example, ordered hierarchical hybrid structures containing both mesopores and macropores in a single solid are expected to offer a high number of accessible reactive sites (due to large specific surface area of the mesoporous part) along with fast mass transport issues (thanks to the interconnected macroporous framework). It is now well-established that ordered mesoporous materials can be generated by soft-templating approaches,[6] and significant progress emerged recently in the preparation of three-dimensionally ordered macroporous solids by colloidal crystal templating.[2] These two concepts can be combined using sol−gel chemistry, that is, by infiltration of a sol solution containing both precursors and a molecular template into void volumes defined by spatially arranged closed-packed colloidal crystals (e.g., polymer beads) and subsequent gelification in the form of a regular macroporous−mesoporous bimodal structure.[7,8] The careful arrangement of templates displaying various sizes allows then the production of materials with multiscale porosity, microporous, mesoporous, and macroporous.[9,10] Such an approach was essentially applied to the preparation of materials in the form of monoliths or powders, whereas thin films with hierarchical porosity are much less described,[11] probably due to the difficulty to combine evaporation methods of sol−gel deposition with colloidal crystal assemblies deposited onto solid surfaces.

The thin film configuration is, however, extremely important for various applications.[9,12] To date, electrochemistry has proven to be efficient to generate hierarchical nanoporous structures such as macroporous−mesoporous Pt deposits via electroreduction of H_2PtCl_6 through colloidal crystal assemblies in the presence of a surfactant template[13] or porous silicon by electrochemical anodization.[14]

*Corresponding author. Tel: +33 (0)3 83 68 52 50. Fax: +33 (0)3 83 27 54 44. E-mail: etienne@lcpme.cnrs-nancy.fr.

(1) Yuan, Z.-Y.; Su, B. L. *J. Mater. Chem.* **2006**, *16*, 663.
(2) Lytle, J. C.; Stein, A. In *Annual reviews of nano research*; Cao, G., Brinker, C. J., Eds.; World Scientific Publishing Co. Pte. Ltd.: Singapore, 2006; Vol. *1*, pp 1−79.
(3) Thomas, A.; Goettmann, F.; Antonietti, M. *Chem. Mater.* **2008**, *20*, 738.
(4) Tao, S.; Shi, Z.; Li, G.; Li, P. *ChemPhysChem* **2006**, *7*, 1902.
(5) Antonietti, M.; Ozin, G. A. *Chem.—Eur. J.* **2004**, *10*, 28.
(6) Wan, Y.; Zhao, D. *Chem. Rev.* **2007**, *107*, 2821.
(7) Holland, B. T.; Abrams, L.; Stein, A. *J. Am. Chem. Soc.* **1999**, *121*, 4308.
(8) Luo, Q.; Li, L.; Yang, B.; Zhao, D. *Chem. Lett.* **2000**, 378.
(9) Sanchez, C.; Boissière, C.; Grosso, D.; Laberty, C.; Nicole, L. *Chem. Mater.* **2008**, *20*, 682.
(10) Sel, O.; Kunag, D. B.; Thommes, M.; Smarsly, B. *Langmuir* **2006**, *22*, 2311.
(11) Sel, O.; Sallard, S.; Brezesinski, T.; Rathousky, J.; Dunphy, D. R.; Collord, A.; Smarsly, B. M. *Adv. Funct. Mater.* **2007**, *17*, 3241.
(12) Walcarius, A.; Kuhn, A. *Trends Anal. Chem.* **2008**, *27*, 593.
(13) Yamauchi, Y.; Kuroda., K. *Electrochem. Commun.* **2006**, *8*, 1677.
(14) Granitzer, P.; Rumpf, K.; Poelt, P.; Reichmann, A.; Krenn, H. *Physica E: Low-Dimensional Systems & Nanostructures* **2007**, *38*, 205.

 Published on Web 05/10/2010

No example of electro-assisted deposition of macroporous or hierarchical silica films has been reported to the best of our knowledge, and we demonstrate here that such an approach can be applied to prepare ordered sol−gel thin films exhibiting both macropores and mesopores. Among other advantages, the method permits growth of the film from the electrode substrate, which induces a good connection between the sol−gel material and the electrode. The electrochemical deposition of silica by the sol−gel process was introduced a decade ago by Shacham et al.[15] It involves the application of a suitable cathodic potential to an electrode immersed in a hydrolyzed sol solution to generate the hydroxide ions[16] that catalyze the precursors polycondensation to form a silica network as a thin film onto the electrode surface. This method was then extended to the generation of organically functionalized silica films.[17] We have recently shown that such electro-assisted deposition can be advantageously combined with the surfactant templating process to generate highly ordered mesoporous silica films with unique mesopore orientation normal to the underlying support,[18,19] and this was also exploited to prepare vertically aligned silica mesochannels bearing organo-functional groups.[20]

Here, we describe an electrochemical route to synthesize ordered silica gel thin films with combined macropores and mesopores. The method is simple and versatile, and the time scale of the deposition process is short, being on the order of tens of seconds only, which is well compatible with the mesostructuration occurring by combination of the electrochemically driven self-assembly of surfactants at solid/liquid interfaces and the sol−gel transition. In the present study, the sol composition and time of deposition were optimized to obtain homogeneous films with defined porosity. The materials characteristics and properties were determined using various physicochemical techniques to get insight in their structure and morphology as well as to discuss the effect of multiscale porosity on molecular transport through the films.

2. Experimental Section

2.1. Chemicals and Reagents. Styrene (Aldrich, reagent plus >99%), hexadecane (Flüka, >98%), potassium persulfate (Flüka, >99%), tetraethoxysilane (TEOS, 98%, Alfa Aesar), ethanol (95−96%, Merck), $NaNO_3$ (99%, Fluka), HCl (37%, Riedel de Haen), cetyltrimethylammonium bromide (CTAB, 99%, Acros), potassium hexacyanoferrate(III) ($K_3Fe(CN)_6$, Flüka), ruthenium trispipyridyl ($Ru(bpy)_3^{2+}$, Acros), and potassium hydrogen phthalate (KHP, Flüka) were used as received. All solutions were prepared with high purity water (18 MΩ cm^{-1}) from a Millipore milli-Q water purification system.

2.2. Preparations. Polystyrene (PS) beads (100 nm as average diameter) were synthesized from the literature[21] by inverse emulsion polymerization using chemicals in the following amounts: 6 g of styrene, 250 mg of hexadecane, 334 mg of potassium persulfate, and 24 g of distillated water. The suspension has been filtrated to remove unwanted aggregates and thus to get an aqueous suspension with 20% of PS as the weight ratio.

PS colloidal crystals have been dip-coated on indium tin oxide (ITO) plates (surface resistivity = 8−12 Ω, Delta Technologies) using the above aqueous suspension of PS beads with a withdrawal rate of 4.8 cm·min^{-1} and humidity below 25%.

A typical sol for electrodeposition consisted of 20 mL of ethanol and 20 mL of aqueous solution of 0.1 M $NaNO_3$ to which 6.8 mmol TEOS and 2.2 mmol CTAB were added under stirring. A total of 480 μL of HCl was added to reach a pH close to 3, and the sol was stirred for 2.5 h. After immersion of the electrode covered with the PS bead assembly into the sol, a cathodic potential of −1.3 V versus a silver quasi reference electrode was applied for periods ranging from 10 to 20 s. The electrode was then quickly removed from the solution and immediately rinsed with distilled water. Aging was done overnight at 80 °C, and then temperature was increased by 2 °C/min until reaching 550 °C; this temperature was maintained for 4 h to remove the template. This treatment allows first the mechanical stability of the silica backbone to be increased and then the PS beads and the surfactant template to be removed.

2.3. Instrumentation and Analytical Procedures. The film morphology was characterized by transmission electron microscopy (TEM) using a Philips CM20 microscope at an acceleration voltage of 200 kV. The samples were prepared by mechanically removing some pieces of the films which were then supported on a carbon-coated copper grid. FE-SEM images were obtained using a Stereoscan 440 SEM apparatus (LEICA) having a 4.5-nm resolution.

The film structure was characterized by X-ray diffraction (XRD) in Bragg−Brentano geometry using a Panalytical X'Pert Pro diffractometer operating with a copper cathode ($\lambda_{K\alpha_1}$ = 1.54056 Å) and by grazing-incidence X-ray diffraction (GIXD) using a Nonius Kappa CCD diffractometer equipped with an ApexII CCD detector (copper cathode ($\lambda_{K\bar{\alpha}}$ = 1.54184 Å).

All electrochemical measurements were carried out at room temperature with an Autolab PGSTAT-12 potentiostat (Eco Chemie). Experiments were carried out in a three-electrode cell using a stainless steel counter-electrode and a Ag/AgCl reference electrode. Quantitative analysis of permeability through the mesoporous silica films was performed by hydrodynamic amperometry using a home-built wall-jet electrochemical setup.[26] It consisted of a syringe needle positioned 1 mm from the analyzed film, perpendicular to the film surface (pointing to the center of the electrode surface area defined by a seal (0.4 cm inner diameter)). A platinum wire and an Ag/AgCl reference (Metrohm) complete the device. Volume flow rates (V) were controlled by a peristaltic pump.

Kr adsorption at 77 K was carried out by an automated gas sorption station Autosorb1MP, Quantachrome Corporation, Boyton Beach, FL. The SiO_2 electrodeposited ITO glasses were sliced in small plates and outgassed at 120 °C for 6 h before the measurement. The total volume of analyzed material was 2×10^{-4} cm^3 (surface: 5 cm^2; thickness 4×10^{-5} cm, neglecting the volume occupied by the PS beads).

(15) Shacham, R.; Mandler, D.; Avnir, D. *Adv. Mater.* **1999**, *11*, 384.
(16) Therese, G. H. A.; Kamath, P. V. *Chem. Mater.* **2000**, *12*, 1195.
(17) Sibottier, E.; Sayen, S.; Gaboriaud, F.; Walcarius, A. *Langmuir* **2006**, *22*, 8366.
(18) Walcarius, A.; Sibottier, E.; Etienne, M.; Ghanbaja, J. *Nat. Mater.* **2007**, *6*, 602.
(19) Goux, A.; Etienne, M.; Aubert, E.; Lecomte, C.; Ghanbaja, J.; Walcarius, A. *Chem. Mater.* **2009**, *21*, 731.
(20) Etienne, M.; Goux, A.; Sibottier, E.; Walcarius, A. *J. Nanosci. Nanotechnol.* **2009**, *9*, 2398.
(21) Landfester, K.; Willert, M.; Antonietti, M. *Macromolecules* **2000**, *33*, 2370.

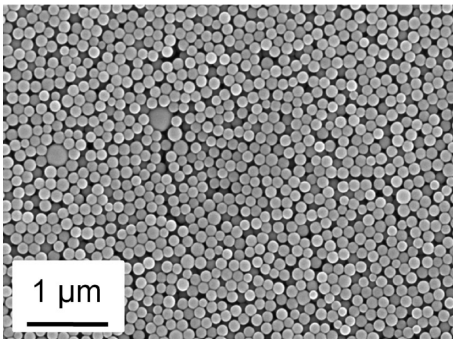

Figure 1. SEM picture of the PS bead assembly, before sol−gel deposition.

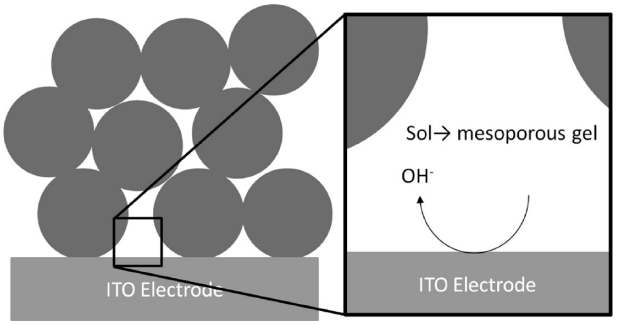

Figure 2. Schematic draw showing the principle of electrochemical generation of macroporous−mesoporous silica.

3. Results and Dsicussion

3.1. Macroporous Texture. Sol−gel silica films were grown on ITO electrodes covered by an assembly of PS beads of 100 nm in diameter (see SEM picture in Figure 1). The layer thickness of the polymer bead assembly can be adjusted by changing the bead concentration in the suspension and the dip-coating conditions. The layers used as template for electrochemical deposition were 600 to 1000 nm thick. ITO-PS was then inserted in the electrodeposition cell and put in contact with the starting sol, typically composed of the alkoxysilane precursors, water, ethanol, HCl, and cetyltrimethylammonium bromide (CTAB) as the molecular template. Gelification was initiated by applying a cathodic potential likely to increase pH from its starting value of 3 to values higher than 9 at the electrode/solution interface by reduction of protons, nitrate and water molecules. The CTAB concentration in the sol was adjusted above the critical micellar concentration (∼30 mM).[22] Under these conditions, the gelification induces the formation of a mesoporous silica network growing from the electrode surface through the void volumes of the polymer nanoparticles assembly (see illustrative scheme of the process in Figure 2).[19] Finally, the porous material was obtained by calcinations at 550 °C.

Scanning electron micrographs (SEM) depicted in Figure 3 demonstrate successful deposition and show the influence of the deposition time, from 10 to 20 s, on the film aspect on the basis of both top and cross-sectional views. Short time deposition (10 s) only led to limited growth of the film, which means that only two or three bead layers have been filled with the silica gel and the bead shape was hardly observable. The top-view of a film deposited for 13 s shows a quite similar morphology but displays a higher material density. Here, spherical shapes and interconnections (originating from PS beads dissolution) are clearly visible. Note that all SEM pictures depicted in Figure 3 have been obtained from metalized samples, and this treatment (useful to get images with good resolution) might result in some distortion of the real appearance of the microstructures. A control experiment without metallization has thus been performed on the 13-s deposited sample, confirming unambiguously the homogeneous deposit of macroporous silica as inverse

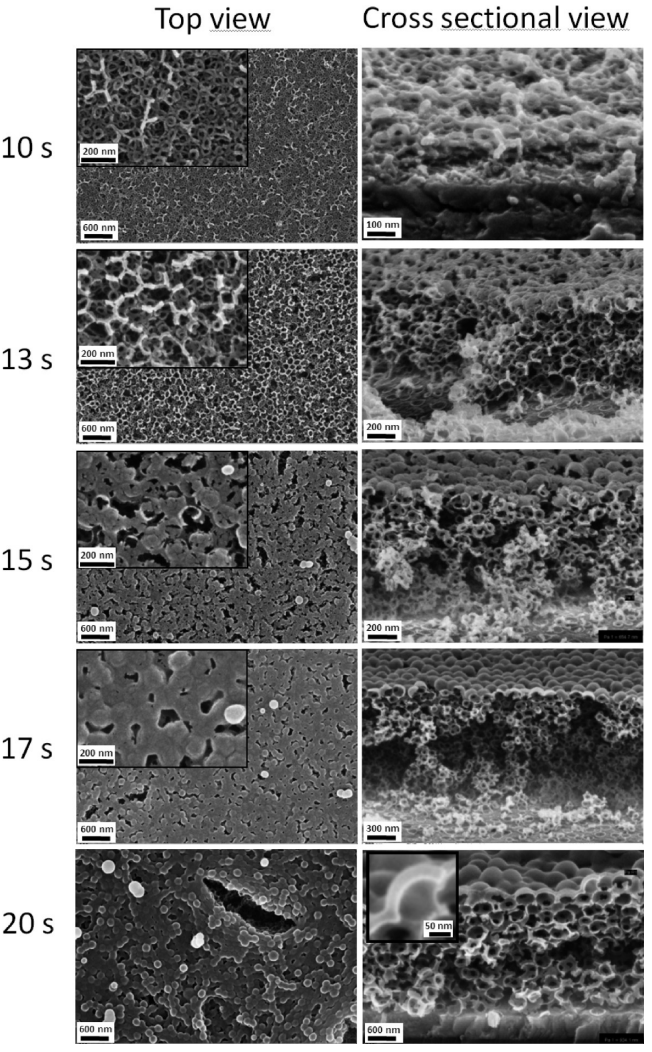

Figure 3. FE-SEM picture showing cross sectional and top views of films formed with electrodeposition time from 10 to 20 s.

opals, in spite of a lower resolution compared to metalized samples (see Figure SI 1 in Supporting Information). Increasing the deposition time to 15 s led to a further densification of the silica matrix and to the complete coverage of the PS beads, while small defects were still present in the top layer. Deposition times of 17 and 20 s allowed forming a dense material (i.e., resulting from dense packing of the silica shell around PS beads), as seen on the top view. In parallel to the densification of the whole layer,

(22) Li, W.; Han, Y. C.; Zhang, J. L. *Colloid J.* **2005**, *67*, 159.

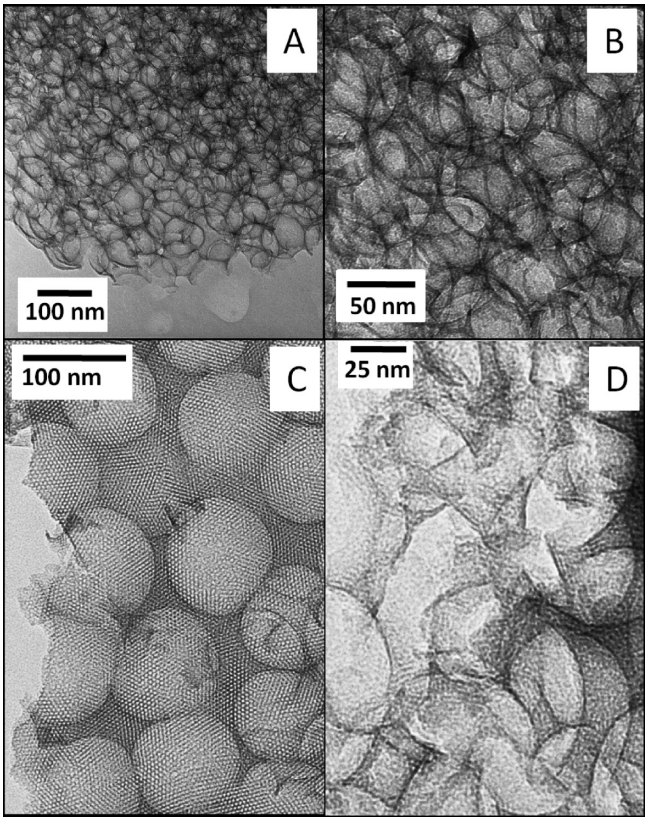

Figure 4. TEM picture of fragments of films deposited for 13 s (A and B) and 17 s (C and D).

increasing deposition time from 17 to 20 s also resulted in a further growth of the top layer of the macroporous film, which is characterized by a thickness of the upper silica walls increasing from about 20 to 40 nm (the thicker walls obtained for the 20-s deposit are shown in the enlarged view of the film cross-section, see inset in the right lower part of Figure 3). Shrinkage into the film was only observed for the longer deposition time with the presence of cracks into the film deposited with using 20 s electrolysis. A significant distortion of the macropores can also be evidenced on the SEM images.

3.2. Mesoporous Texture. Transmission electron microscopy (TEM) was then applied to evidence the mesoporous parts of the films. Figure 4 displays a set of TEM pictures showing details of electrogenerated films by applying respectively short (A and B) and long (C and D) electrolysis times. For short periods of electrolysis (13 s, Figure 4A,B) relatively thin walls were observed between the macropores. The macropore size corresponds to the diameter of the PS bead template, being in the range of 100 nm. Figure 4C shows the top view of a sample obtained after 17 s of deposition, that is, a longer period of time, revealing a very well ordered hexagonal mesostructure and macropores. Looking more inside the macroporous layer revealed also the presence of mesopores (Figure 4D). These results suggest that the thin layer (20−40 nm) formed on the top of the deposit displays a well ordered mesostructure normal to the underlying support, which is confirmed by the high resolution cross-sectional view of this top layer (see Figure 5). It is quite remarkable to observe the same vertical orientation of

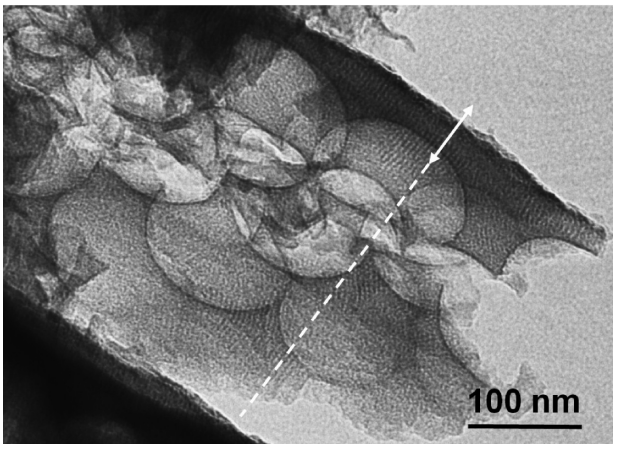

Figure 5. Cross-sectional view obtained with TEM. The arrow indicates the direction normal to the substrate.

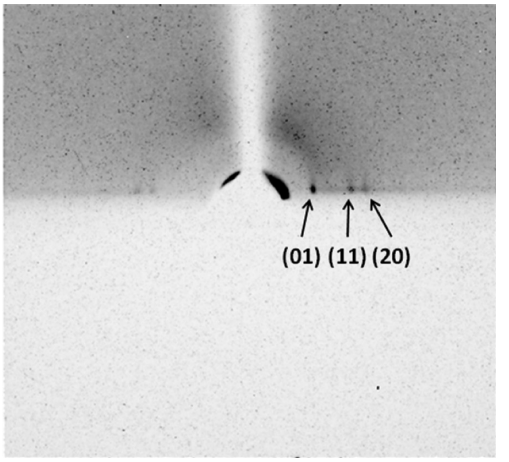

Figure 6. GIXD pattern obtained in the presence of thin silica layer deposited over PS bead assembly for 16 s.

mesopore channels on the top of the PS bead assembly, that is, at a distance about 600−1000 nm from the support, as that reported for oriented mesoporous silica films directly generated on a flat electrode surface.[18,19]

The presence of this oriented mesoporous layer was confirmed by small-angle X-ray scattering at grazing incidence, via diffraction signals of small intensity observed in the equatorial plane (Figure 6). In spite of the low intensity due to the very small amount of analyzed matter, this diffraction pattern can be assigned to a hexagonal mesostructure normal to the electrode substrate on the top of the silica film observed in Figure 4C. For the same reason, diffraction signals can only be observed in case of a sufficiently thick top layer. Attempts to evidence mesostructural order by X-ray scattering analysis in the Bragg−Brentano mode in the underlying macroporous part of the film failed, despite the observation of this mesostructure in TEM images, which can be explained by two possible reasons. First, the quantity of matter within the thin silica layers containing the mesopores was too low and the ordered domain too small to get measurable diffraction signals. A second possibility could be an orientation of the mesopores leading to off-specular Bragg reflections, which would be the case if mesopore channels are all

oriented normal to the underlying support, which constitutes a plausible hypothesis regarding the cross-sectional TEM picture (Figure 5). Finally, in agreement with the above discussion, no detectable diffraction signals were obtained for the films generated at low deposition times.

The surface area and pore volume corresponding to the macropores can, in principle, be determined by Hg porosimetry. However, this technique requires an amount of approximately 150 mg at minimum for a reasonable analysis and could not be done here. Kr adsorption at 77 K can be obtained with a much lower quantity of matter and has been performed on a film deposited for 13 s. This measurement allowed the determination of the BET surface area of the mesoporous part of the material, which resulted to be 61 m^2/cm^3. According to the standard procedure, the saturation pressure of the supercooled Krypton ($p^0 = 2.6$ Torr) and the cross sectional area of 20.5 $Å^2$ were used for the calculation.[23] The BET plot was performed in the linearity region $0.05 \leq p/p^0 \leq 0.22$.

Thus, four different steps of sol−gel electrodeposition into the macroporous structure formed by PS bead assembly can be resumed (see scheme in Figure 7). (A) During the first seconds of deposition, only a thin silica layer is formed around the PS beads. This behavior has been already described for TiO_2 electrodeposition[24] and agrees well with faster precursor polycondensation onto solid surfaces in comparison to bulk gelification from homogeneous sols.[25] Only a portion of the PS beads are covered by silica. (B) For longer deposition time, PS beads remain covered by a thin silica layer, but almost all beads become covered with silica. (C) Further deposition leads to a more complete filling of the voids between the PS particles. (D) In the last step of the process, the macroporous texture is formed and mainly the top layer of the macroporous film continues growing. As aforementioned, the top layer displays well ordered mesopores oriented normal to the electrode substrate.

3.3. Electrochemical Characterization. Electrochemical methods are not only suitable for synthesis but also very useful to characterize mass transport issues through porous layers, as previously shown for mesoporous silica thin films of various mesostructure types deposited onto electrode surfaces.[26] Cyclic voltammetry (CV) was first applied to get qualitative information. Experiments were performed with films deposited using 13 s electrolysis, of course after template extraction, using two distinct redox probes; $Fe(CN)_6^{3-}$ (Figure 8A) or $Ru(bpy)_3^{2+}$ (Figure 8B). The experiments have been performed in potassium hydrogen phthalate solution 0.05 M at pH 4.1 for preventing silica dissolution during the analysis.[27] Three different curves are reported, the electrochemical response

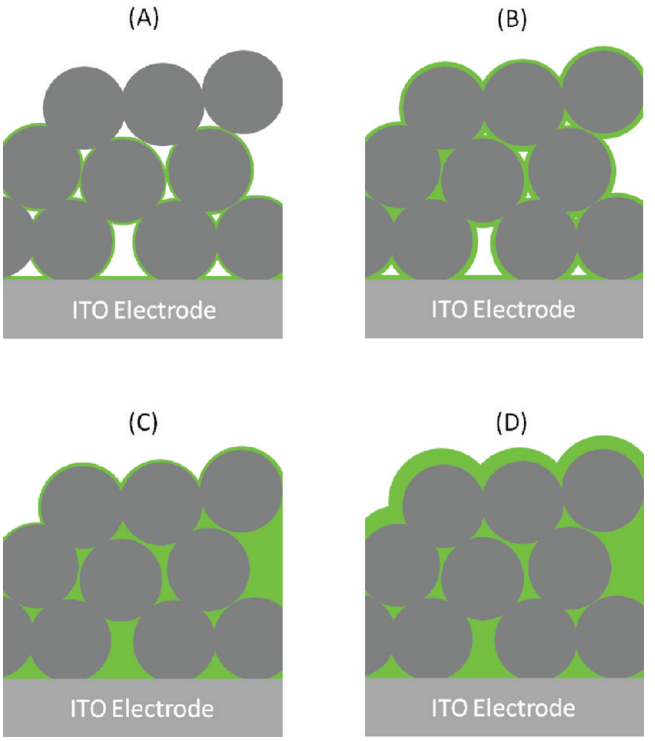

Figure 7. Different steps that have been observed during electrochemical deposition of mesopores on the PS bead assembly. (A) Thin layer formation on a limited height, (B) thin silica layer on all layers of PS beads, (C) densification of the matrix, and (D) growth of a top layer over the PS bead assembly.

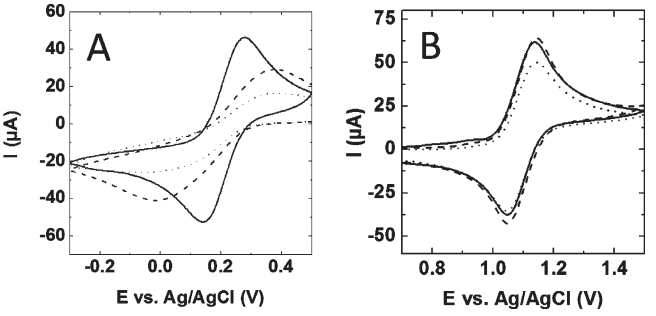

Figure 8. Cyclic voltammograms obtained in the presence of 1 mM $Fe(CN)_6^{3-}$ (A) or $Ru(bpy)_3^{2+}$ (B) on ITO electrode (plain line) and ITO electrode modified with a bimodal macroporous−mesoporous film (dashed line) or a mesoporous film (dotted line).

of the bare electrode (plain line), the response observed in the presence of a purely mesoporous silica film (i.e., prepared with the CTAB but without colloidal crystal template, dotted line) and that in the presence of the bimodal macroporous−mesoporous film (dashed line). CVs in the presence of the negatively charged $Fe(CN)_6^{3-}$ probe clearly show that the silica films induce some limitations of the electrochemical process as characterized by lower peak current intensities and higher peak-to-peak potential separations. This limitation results from resistance to mass transport, which is accentuated by electrostatic repulsions between the negative probe and the negatively charged silica surface.[27] As shown, the bimodal film leads to a higher electrochemical response than the mesoporous film, suggesting that the presence of interconnected

(23) Gregg, S. J.; Sing, K. S. W. *Adsorption, Surface Area and Porosity*; Academic Press: London, 1982.
(24) Xu, Y.; Zhu, X.; Dan, Y.; Moon, J. H.; Chen, V. W.; Johnson, A. T.; Perry, J. W.; Yang, S. *Chem. Mater.* **2008**, *20*, 1816.
(25) Brinker, C. J.; Gong, W.; Guo, Y.; Soyez, H.; Dunn, B.; Huang, M. H.; Zink, J. I. *Nature* **1997**, *389*, 364.
(26) Etienne, M.; Quach, A.; Grosso, D.; Nicole, L.; Sanchez, C.; Walcarius, A. *Chem. Mater.* **2007**, *19*, 844.
(27) Song, C.; Villemure, G. *Microporous Mesoporous Mater.* **2001**, *44−45*, 679.

macropores clearly improves the access to the electrode surface. CV curves recorded in the presence of $Ru(bpy)_3^{2+}$ do not display such strong differences between the three electrodes, most probably because resistance to mass transport is hidden by the possible accumulation of the positively charged probe onto the silica surface via attractive interactions with silanolate groups.[18,26] A slight increase in peak current intensities is observed with the bimodal film, which could be due to a better preconcentration of $Ru(bpy)_3^{2+}$ into the macroporous−mesoporous material.

More quantitative characterization of mass transport can be achieved by using wall-jet electrochemistry (WJE), a technique developed for permeability measurements through thin films deposited on flat electrode surfaces,[28] which has been already successfully applied to mesoporous silica thin films.[26] It is based on the electrochemical oxidation (or reduction) of an electroactive probe likely to diffuse through the layer, under controlled convection. (i.e., measurement of effective kinetic constants, k_{eff} values). Such measurement should provide here further insight in the hierarchy between different porous films, that is, the macroporous−mesoporous bimodal film developed in the present study, a macroporous film prepared using colloidal crystal templating only (without surfactant and thus exhibiting no mesoporosity; its SEM picture is shown in Supporting Information Figure SI 2), and a pure mesoporous silica film (without macroporosity). The electrochemical data are shown in Figure 9 while the corresponding k_{eff} values calculated from these data are gathered in Table 1.

They clearly show that the underlying ITO electrode surface remains accessible to the probe ($Ru(bpy)_3^{2+}$) for all films, but the effective rate constant depended strongly on the porosity of the deposited layer. The value for the mesoporous−macroporous film (3.8×10^{-2} cm s^{-1}) was higher than the mesoporous one (1.4×10^{-2} cm s^{-1}), very close to the macroporous system (1.3×10^{-2} cm s^{-1}). The improved behavior of the bimodal film is certainly due to the interconnection between macropores, which can be facilitated by the existence of mesopores in the silica shells, by comparison to the film only composed of macropores (non- or poorly porous shells).

Assuming the diffusion into a membrane-like layer, it is possible to extract the permeability (PD_f) from the effective kinetic constant, according to eq 1:

$$k_{eff} = PD_f/d \quad (1)$$

where P is the partition coefficient between the solution and the film, D_f the apparent diffusion coefficient through the film (cm^2 s^{-1}), and d the thickness of the layer (cm). With this hypothesis we found permeability values of about 2×10^{-6} cm^2 s^{-1} for the bimodal mesoporous−macroporous film. This value is significantly higher than the one found for a mesoporous film prepared with the same deposition time (4×10^{-8} cm^2 s^{-1}) and is very close to the diffusion coefficient of the molecular probe in solution (2.6×10^{-6} cm^2 s^{-1}), demonstrating that the electrogenerated mesoporous−macroporous layers developed in this study provide attractive features in terms of low limitation for the diffusion of molecular probes.

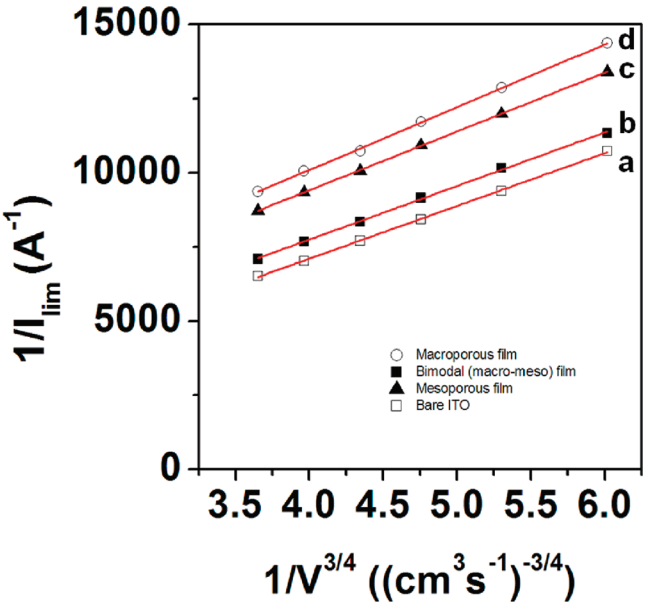

Figure 9. $1/I$ versus $1/V^{3/4}$ for (a) bare ITO electrode and ITO electrode modified by (b) bimodal macroporous−mesoporous film, (c) mesoporous film, and (d) macroporous film.

Table 1. Electrochemical Data Characterizing Transport Properties through Thin Films (using $Ru(bpy)_3^{2+}$ as the redox probe)

sample	macroporous−mesoporous[a]	mesoporous[b]	macroporous[a]
k_{eff} (cm s^{-1})	3.8×10^{-2}	1.4×10^{-2}	1.3×10^{-2}
PD_f (cm^2 s^{-1})	2×10^{-6}	4×10^{-8}	7×10^{-7}

[a] $d \sim 600$ nm. [b] $d \sim 30$ nm.

4. Conclusion

In summary, we show here for the first time that silica gel layers with hierarchical porosity can be prepared on electrode surfaces by electro-assisted deposition. Macropores and mesopores are produced by PS beads and CTAB micelles templates, respectively. The filling of voids between the PS bead template strongly depends on the deposition time. Low deposition time leads only to the deposition of a very thin silica layer on the PS beads. Longer deposition time leads to the complete filling of the macroporous texture and to the growth of an additional layer with very well oriented pores normal to the electrode surface. The hierarchical material is highly permeable to external reagents, being thereby promising for various applications involving such mass transport processes. This work opens an interesting outlook for the electrodeposition of sol−gel type materials with finely tuned porosity and reactivity.

Acknowledgment. This work was supported by PHC-PROCOPE and partially funded by the European Community through the ERUDESP project (FP7-NMP 213 487). We are

(28) Massari, M.; Gurney, R. W.; Schwartz, C. P.; Nguyen, S. B. T.; Hupp, J. T. *Langmuir* **2004**, *20*, 4422.

also grateful to J. Ghanbaja for TEM experiments, S. Borensztajn for FE-SEM experiments, and E. Wenger for his help with XRD measurements. We thank E. Aubert for GIXD experiment and the Service Commun de Diffraction X, Institut Jean Barriol, Nancy-Université, for providing access to crystallographic facilities.

Supporting Information Available: SEM image of the electrodeposited silica film with hierarchical porosity obtained without platinum metallization. SEM picture of a macroporous silica film. Additional TEM images of the hierarchical material are also provided (PDF). This material is available free of charge via the Internet at http://pubs.acs.org.